



OPEN Repeatability of Scheimpflug-Placido camera in mild dry eye versus normal eyes according to the topographical position of the cornea

Sunjin Hwang^{1,2}, Dae Sung Kim^{3,4}, Duroo Kim^{1,2}, Eun Hee Hong^{1,2}, Yong Un Shin^{1,2}, Yu Jeong Kim^{1,3} & Min Ho Kang^{1,2}✉

We aimed to investigate the repeatability of various corneal measurements according to topographical location in the entire cornea measured by dual rotating Scheimpflug-Placido camera and to explore the differences in repeatability between patients with mild dry eye and those with normal eyes. In both the normal and dry eye groups, divided based on BUT or the height of the tear film, there were no statistically significant differences in the ratio of unacceptable variation (RUV) and ICC. The consistency of the examination of the anterior and posterior refractive values and corneal thickness according to the corneal location, measured three times repeatedly using the Galilei anterior segment camera, was high. There was no difference based on the height of the tear film or the tear film break-up time. However, caution is needed when interpreting the values of the anterior corneal refractive values, as there can be changes of more than 0.5D within 3 mm of the central area.

Accurately determining corneal power is crucial for intraocular lens specifications and astigmatism correction surgeries, while corneal wavefront aberrations guide custom laser ablation treatments. Additionally, evaluating corneal thickness is pivotal for assessing refractive surgery candidacy, aiding in surgical planning, and determining suitability for procedures like corneal cross-linking and intrastromal corneal ring segment insertion¹⁻³.

Devices employing Scheimpflug imaging for the anterior segment offer enhanced accuracy by assessing both anterior and posterior corneal curvatures^{4,5}. The Galilei G6 Dual Scheimpflug camera (Ziemer USA, Wood River, IL) employs a dual-channel system with rotating Scheimpflug cameras and a placido disk, providing comprehensive measurements and maps of anterior and posterior corneal curvature, corneal thickness, and corneal power. The simultaneous use of dual cameras ensures reliable data on corneal thickness and posterior corneal curvature, while incorporating placido disk data enhances topographic analysis of anterior corneal curvature⁶.

Evaluating the clinical utility of diagnostic devices necessitates understanding potential test errors and the accuracy of repeated measurements. Factors such as tear film condition and eye pressure can affect corneal topography accuracy^{7,8}. Previous studies have shown the Galilei's high repeatability in assessing corneal power and thickness, albeit primarily focusing on central corneal measurements^{5,6,9-11}. This study aims to investigate the repeatability of various corneal measurements across topographical locations using the Galilei. Additionally, we aim to analyze differences in repeatability between patients with mild dry eye and normal eyes to assess the impact of tear film variations.

Methods

This study is a prospective, cross-sectional, observational study that was conducted on patients visiting department of Ophthalmology in Hanyang University Guri Hospital from March to July 2020. The study was approved by the Institutional Review Board of Hanyang University Guri Hospital, in accordance with the principles stated in the Declaration of Helsinki (IRB number 2020-05-013-009). All patients provided fully written informed consent after receiving the description of the study. Patients with normal eyes and those with dry eye disease

¹Department of Ophthalmology, Hanyang University College of Medicine, Seoul, Korea. ²Department of Ophthalmology, Hanyang University Guri Hospital, Guri, Korea. ³Department of Ophthalmology, Hanyang University Hospital, Seoul, Korea. ⁴Blue Eye Center, Paju, Korea. ✉email: bsdoc@hanyang.ac.kr

(the criteria for diagnosing dry eye disease did not include subjective symptoms, instead, it classified dry eye and normal based on a BUT of less than 5 s or a TMH of less than 150 μm to assess the repeatability due to tears), aged between 20 and 40 years were recruited. It included patients without corneal opacity or keratoconus, and excluded those with a moderate to severe conjunctiva or corneal staining of dry eye syndrome according to the DEWS II classification^{12,13}.

Participants underwent sequential examinations with one eye randomly selected per participant. Examinations were conducted at least one hour after the last application of artificial tears to minimize tear film influence. Patients were instructed to blink before measurements, conducted in a darkened room. A single experienced examiner performed three measurements per eye within 30-min period to eliminate normal diurnal variations of corneal curvature and thickness¹⁴. The tear meniscus height (TMH) on the lower eyelid below the central cornea was measured using anterior segment optical coherence tomography (Topcon, Tokyo, Japan), and the average of the values manually measured by different observers (S.H. and M.H.K) was used. The anterior and posterior curvature radii and corneal thickness of the cornea were measured using a Galilei G6 (Ziemer USA, Wood River, IL). The Galilei provides quality score, and poor-quality score was abandoned and performed again until it reaches the favorable quality score. The anterior segment photography was performed three times consecutively. Fluorescein tear film break-up time (BUT) was measured by dropping 5 μl of 0.1% fluorescein into the lower conjunctival sac, then opening and closing the eyes several times, and the average of three consecutive measurements was used.

The anterior segment camera was able to obtain test values for 18,002 corneal locations at each measurement, and a color map was obtained using MATLAB[®] R2020a (The MathWorks, Inc., Natick, Massachusetts, United States) (Fig. 1). Galilei provides raw data for each point on the cornea in a csv file. We loaded this data into MATLAB, and after analyzing the consistency of the values at each location, we coded a color map to obtain the results. In cases where there is a clinically significant differences, the ratio of values exceeding 0.5D in corneal refractive power and more than 25 μm in corneal thickness was defined as the ratio of unacceptable variation (RUV), which is approximately double the threshold values used in Scheimpflug-based topography to determine the progression of keratoconus. This was assessed for anterior axial curvature, posterior axial curvature, and corneal thickness, respectively.

Statistical analysis was performed using SPSS (IBM SPSS Statistics for Windows, Version 27.0. Armonk, NY: IBM Corp) and P values of 0.05 or less were considered statistically significant. Normal eyes and those with dry eye syndrome were classified through BUT and TMH. The differences in the intraclass correlation coefficient (ICC) and the RUV between two groups were analyzed using an independent t-test. Additionally, the correlation between BUT and TMH was examined using Pearson's correlation analysis. Mean of the absolute differences in the anterior and posterior curvature radii and corneal thickness of the cornea according to corneal location was calculated based on three measurements, and an intraclass correlation analysis was performed to evaluate the consistency of the measurements.

Results

A total of 64 eyes were enrolled, comprising 24 from normal participants and 40 from patients with dry eye. Mean age of participants was 26.7 ± 2.4 years, with 17 female patients. Demographic characteristics are summarized in Table 1.

When dividing the participants into normal and dry eye groups based on a BUT of 5 s, there were 24 eyes in the normal group and 40 eyes in the dry eye group, with average BUT of 9.1 ± 2.8 s, and 3.0 ± 1.1 s, respectively ($p < 0.001$). The average TMH was 222.9 ± 73.9 μm for the normal group and 195.7 ± 79.9 μm for the dry eye group, which was not statistically significant ($p = 0.181$). Also, BUT and TMH showed no significant correlation

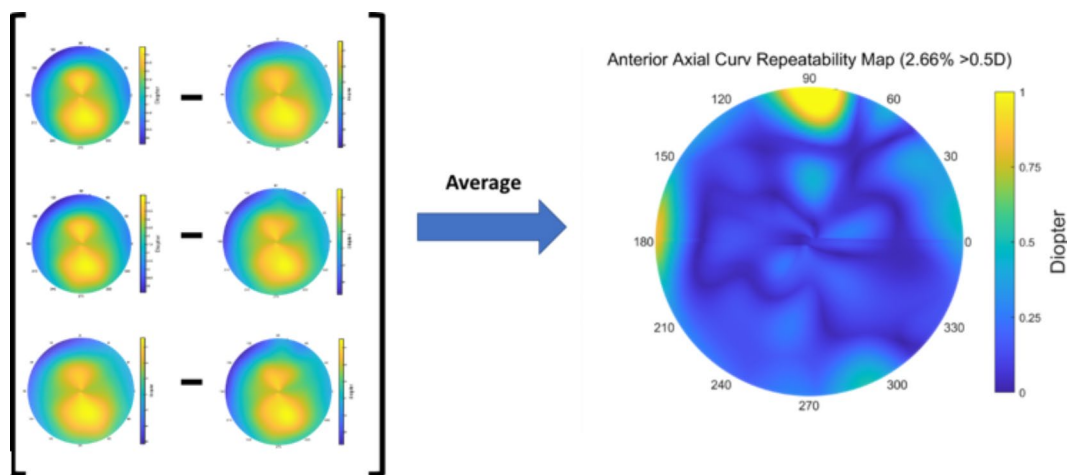


Fig. 1. From the three repetitive measurements taken with the Galilei, values for anterior axial curvature, posterior axial curvature, and corneal thickness were obtained from 18,002 points across the entire cornea. The average of the absolute differences for each of these values was then represented in a color map.

Total	64 eyes
Age (years)	26.7 ± 2.4
Sex (female (number, %))	17, 26.5
TMH (μm)	308.57 ± 77.79
BUT (s)	5.28 ± 3.59
Variation of anterior axial curvature (D)	26.99 ± 17.59
Variation of posterior axial curvature (D)	2.61 ± 3.96
Variation of pachymetry (μm)	2.76 ± 5.62

Table 1. Demographics of patients. BUT, Break-up time ; TMH, tear meniscus height.

	Normal	Dry eye (BUT < 5 s)	P value	
Total patients		24	40	
BUT (s)		9.1 ± 2.8	3.0 ± 1.1	< 0.001
TMH (μm)		222.9 ± 73.9	195.7 ± 79.9	0.181
Ratio of unacceptable variation (%)	Anterior Axial Curvature (D)	6.9 ± 7.9	7.9 ± 7.8	0.634
	Posterior Axial Curvature (D)	0.7 ± 2.0	0.5 ± 1.6	0.616
	Pachymetry (μm)	2.7 ± 6.6	1.6 ± 2.2	0.321
Intraclass correlation coefficient	Anterior Axial Curvature (D)	0.97 ± 0.04	0.98 ± 0.02	0.396
	Posterior Axial Curvature (D)	0.90 ± 0.17	0.94 ± 0.10	0.355
	Pachymetry (μm)	0.99 ± 0.02	0.99 ± 0.003	0.171

Table 2. Results of ratio of unacceptable variation and intraclass correlation in normal and dry eyes when groups with a BUT of less than 5 s were classified as having dry eye. BUT, Break-up time; TMH, tear meniscus height. Significant are in value [bold].

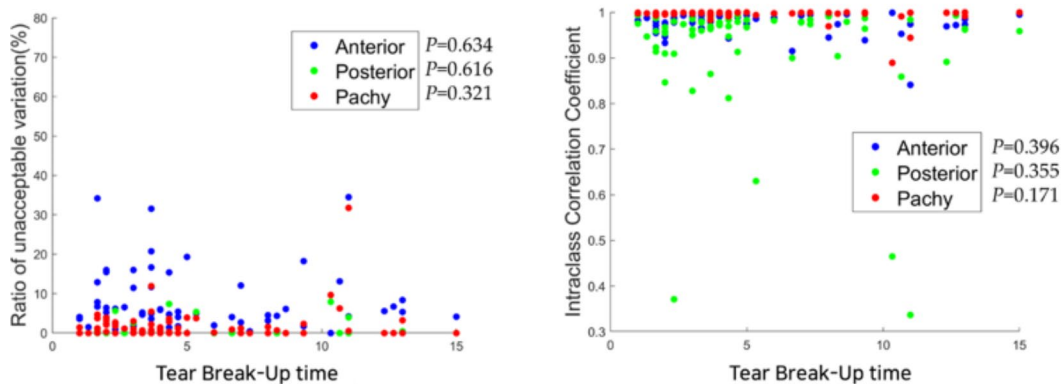


Fig. 2. The ratio of unacceptable variation and the intraclass correlation coefficient for anterior axial curvature, posterior axial curvature, and corneal thickness according to BUT were graphically represented. Blue dots indicate anterior axial curvature, green dots represent posterior axial curvature, and red dots represent corneal thickness. BUT,

($p = 0.225$). Both the RUV and ICC of anterior axial curvature, posterior axial curvature, and corneal thickness showed no significant difference with $p > 0.05$. (Table 2, Fig. 2).

Break-up time

When classified based on a TMH threshold of 150 μm, there were 29 eyes in the normal group and 35 eyes in the dry eye group, with average BUT of 5.39 ± 2.9 s, and 5.18 ± 3.9 s, respectively, showing no significant difference. However, the TMH was 275.1 ± 59.3 μm for normal group and 148.5 ± 31.4 μm for the dry eye group, indicating a statistically significant difference ($p < 0.001$). Even in this classification, both RUV and ICC of anterior axial curvature, posterior axial curvature, and corneal thickness showed no statistically significant differences, with $p > 0.05$ (Table 3, Fig. 3).

	Normal	Dry eye (THM < 150 μm)	<i>P</i> value	
Total patients		29	35	
BUT (sec)		5.39 \pm 2.9	5.18 \pm 3.9	0.814
TMH (μm)		275.1 \pm 59.3	148.5 \pm 31.4	< 0.001
Ratio of Unacceptable variation(%)	Anterior Axial Curvature (D)	7.1 \pm 7.4	7.9 \pm 8.2	0.688
	Posterior Axial Curvature (D)	1.0 \pm 2.3	0.2 \pm 0.9	0.616
	Pachymetry (μm)	2.1 \pm 2.9	1.9 \pm 5.4	0.102
Intraclass correlation coefficient	Anterior Axial Curvature (D)	0.98 \pm 0.02	0.98 \pm 0.03	0.852
	Posterior Axial Curvature (D)	0.90 \pm 0.15	0.94 \pm 0.11	0.177
	Pachymetry (μm)	0.99 \pm 0.02	0.99 \pm 0.01	0.447

Table 3. Results of ratio of unacceptable variation and intraclass correlation in normal and dry eyes when groups with a TMH of less than 150 μm were classified as having dry eye. BUT, Break-up time; TMH, tear meniscus height. Significant are in value [bold].

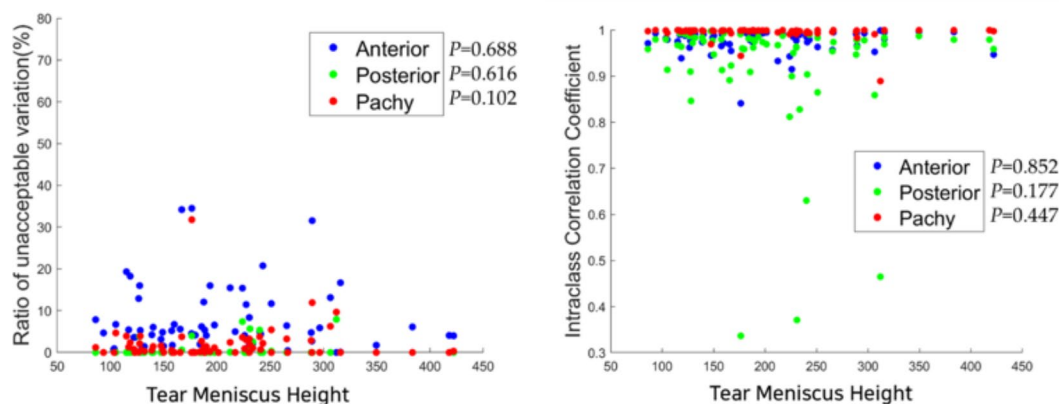


Fig. 3. The ratio of unacceptable variation and the intraclass correlation coefficient for anterior axial curvature, posterior axial curvature, and corneal thickness according to TMH were graphically represented. Blue dots indicate anterior axial curvature, green dots represent posterior axial curvature, and red dots represent corneal thickness.

TMH, tear meniscus height

The repeatability map can be divided into four types: forms with almost no variability; forms with significant anterior refractive changes exceeding 0.5D, but stable posterior refractive values and corneal thickness; forms with significant variability in values other than anterior refractive values; and forms with significant variability in values other than posterior refractive values (Fig. 4).

RUV, Ratio of unacceptable variation

When plotting the angles and positions from the corneal center of the points where the variability was more than 0.5D or 25 μm , it was observed that the anterior axial curvature showed a lot of variability even within 3 mm of the center. In the case of posterior axial curvature and corneal thickness, the central area was stable, but variations could be seen in the peripheral areas of the upper and lower cornea. Additionally, it can be observed that overall, the upper cornea exhibits greater variability compared to the lower cornea (Fig. 5).

Discussion

This study found high repeatability in measurements of anterior and posterior axial curvature, and corneal thickness obtained through repeated Galilei anterior segment camera assessments, regardless of corneal location. Variations in tear film parameters such as BUT and TMH did not affect repeatability. Although RUV was low within the central 3 mm of the cornea for posterior axial curvature and corneal thickness, higher variability was noted in anterior axial curvature within the same region.

It is known that Galilei system showed better repeatability than other devices (Orbscan II or Pentacam)¹⁵. In previous studies, repeatability is typically measured for metrics such as flat keratometry, steep keratometry, or central corneal thickness, which show results localized to the center of the cornea. In this study, using MATLAB, the entire cornea was divided into 18,002 points, and the RUV at each topographically and geographically specific point was measured to assess the repeatability across the whole cornea. While the analysis of the entire cornea showed results that were somewhat consistent with those previously limited to the center in terms of

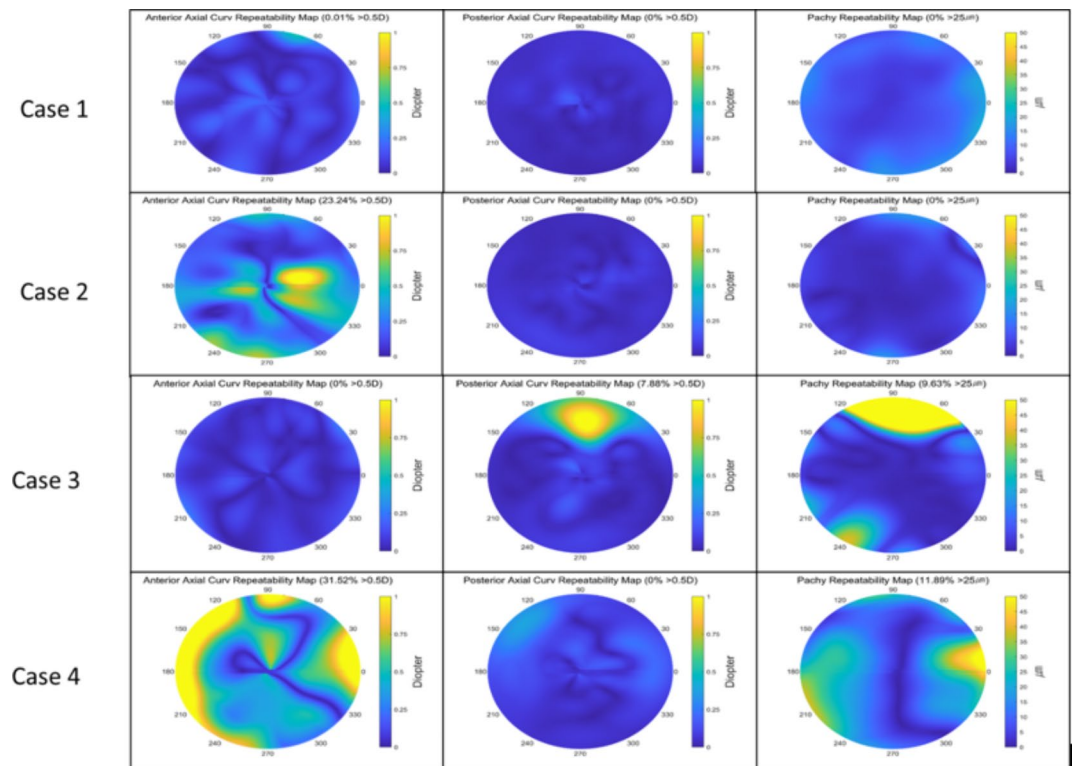


Fig. 4. In the repeatability map, cases where there is a change in corneal refractive power of 0.5D and corneal thickness of 25 μ m, indicating the presence of RUV, were visualized using a color map, and various cases are introduced. The left column represents the color map for anterior axial curvature, the middle column for posterior axial curvature, and the right column for corneal thickness. Case 1 did not show significant variability in anterior axial curvature, posterior axial curvature, or corneal thickness. In Case 2, more than 0.5D of variability in anterior axial curvature was observed in 23.24% of the measurements, particularly in the area 3 mm around the center. Case 3 exhibited significant variability in the posterior axial curvature around the 90-degree area of the peripheral cornea, with a similar pattern observed in corneal thickness. Case 4 revealed substantial variability in the anterior axial curvature in the peripheral regions of the cornea.

repeatability^{16,17}, it was observed that the RUV was significantly present in the center portion in the case of anterior axial curvature.

Although variability in anterior axial curvature is anticipated to be closely related to changes in the tear film⁸, this study did not observe any significant differences among groups divided based on BUT and TMH. Previous study has shown that the pattern of tear film disruption varies with BUT, where linear and dimple breaks occur in mild dry eyes with BUT of 2–3 s, and random breaks occur when BUT exceeds 5 s¹⁸. Given the high ratio of RUV observed within 3 mm of the center of the cornea for anterior axial curvature in this study, it could be inferred that this variability may be due to tear film disruption in the central area.

The upper cornea exhibits greater variability compared to the lower cornea. It can be understood that the differences in the position of the upper and lower eyelids, as well as variations in the tear film's volume and quality in their vicinity, may influence the outcomes. According to the study of ocular surface height analysis¹⁹, there was an observed increase in tear film height at the superior cornea after blinking. This increase is likely due to the swift upward motion of tears following a blink suggesting a localized thickening of the tear film in this area. It is proposed that immediately after a blink, a reduced thickness of the lipid layer at the superior cornea creates higher surface tension, driving the tear film upwards and thickens the tear film in the upper portion of the cornea²⁰. The changes in the tear film of the upper cornea following a blink may potentially contribute to greater variability during measurements. It has been observed that the period 1 to 4 s after a blink offers the highest reliability and minimal influence from the tear film¹⁹, suggesting that considering this timing during examinations could be a strategy to reduce errors.

This study proceeded by randomly selecting one eye from each participant for research. Previous studies^{21–23} have included both eyes of participants, which, while potentially increasing the sample size, introduces a fundamental issue of inter-eye correlation, potentially leading to slight differences in the results.

Previous studies^{24–27} assessing repeatability of Scheimpflug analyzer, typically involved young and healthy participants, which might not fully align with real-world settings. In our study, we focused on a young patient cohort with an average age of 26.7 years and found favorable repeatability outcomes. It is speculated that repeatability might decrease in older patients due to difficulties with eye fixation and lower cooperation levels. However, according to the findings by Kim et al.⁵, examining patients aged 56 ± 18 years (ranging from

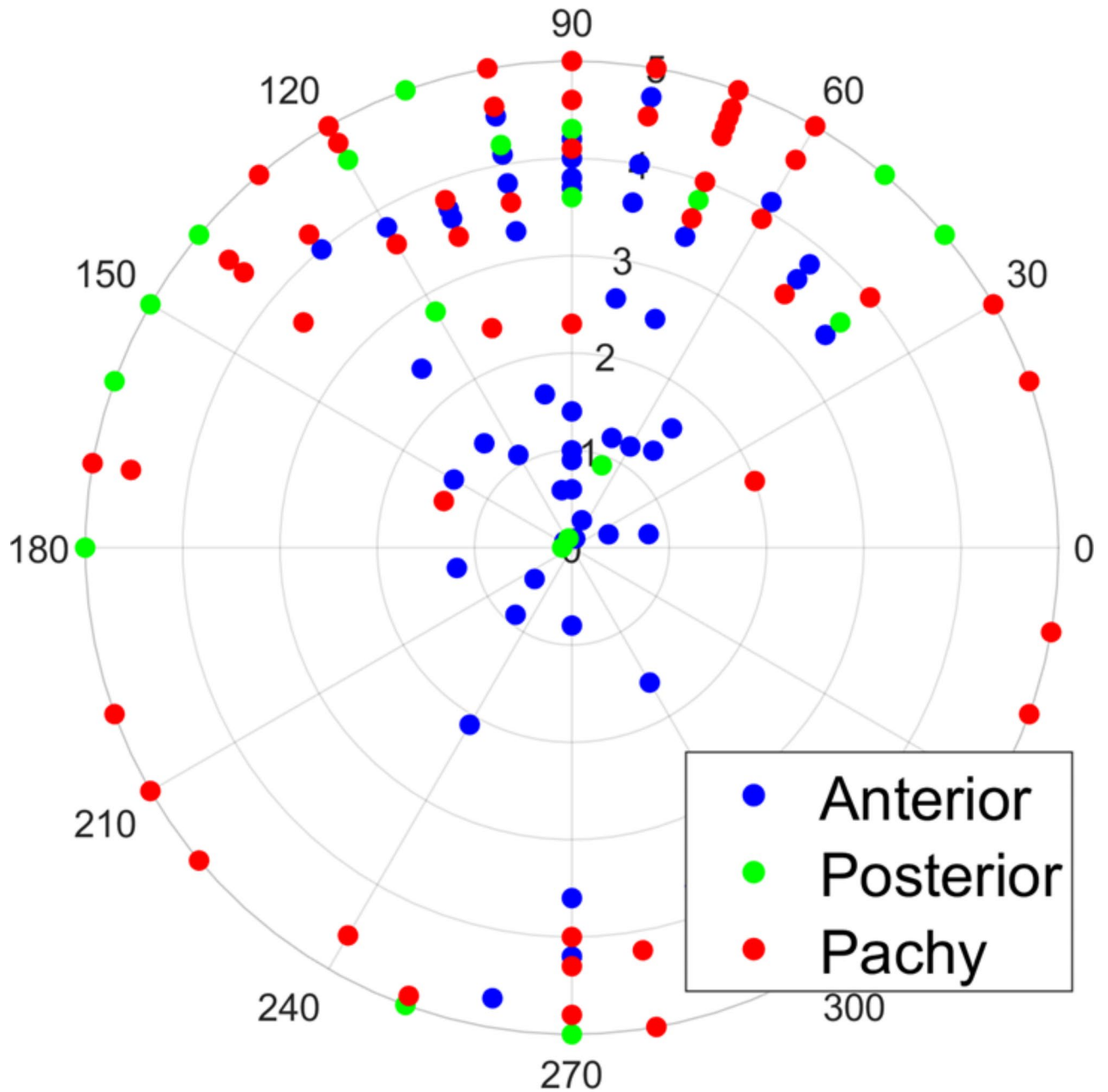


Fig. 5. When plotting the angles and positions from the corneal center of points with variability exceeding 0.5D and 25 μm , it was observed that the anterior axial curvature shows considerable variability even within 3 mm of the center. For posterior axial curvature and corneal thickness, the central areas appeared stable, while variability was noted in the peripheral regions of the upper and lower cornea. Additionally, it can be observed that overall, the upper cornea exhibits greater variability compared to the lower cornea. Blue dots indicate anterior axial curvature, green dots represent posterior axial curvature, and red dots represent corneal thickness. The distance between each ring is 0.9 mm, and the total diameter is 9 mm.

22 to 87 years) revealed repeatability comparable to that of younger participants, indicating that the Galilei demonstrates strong performance in clinical settings.

Our study has some limitations. First, this study did not analyze variations according to the tear film break-up pattern and excluded patients with severe dry eye of grade 2 or above. Second, TMH was manually measured and it might produce some errors. Third, variability between sessions was not examined, and it is anticipated that this factor would also add to the variability observed in the measurements. However, the comprehensive analysis of the entire cornea using MATLAB on 18,002 points represents a strength of this research, as there have been no prior studies analyzing changes across the whole cornea.

In conclusion, this study demonstrated high repeatability of corneal topography measurements obtained through three repeated measurements using the Galilei, with no significant differences observed based on the

BUT and TMH. However, caution should be made when interpreting measurements of anterior axial curvature, especially within 3 mm of the center, due to potential changes exceeding 0.5D. Future research should explore whether variability differs according to the pattern of the tear film disruption, as well as among patients with corneal diseases other than dry eye syndrome, indicating the need for further studies in this area.

Data availability

The datasets used and/or analysed during the current study available from the corresponding author on reasonable request.

Received: 20 May 2024; Accepted: 23 September 2024

Published online: 07 October 2024

References

- Mazzotta, C. & Caragiuli, S. Intraoperative corneal thickness measurement by optical coherence tomography in keratoconic patients undergoing corneal collagen cross-linking. *Am. J. Ophthalmol.* **157**, 1156–1162 (2014).
- Lai, M. M. et al. Optical coherence tomography to assess intrastromal corneal ring segment depth in keratoconic eyes. *J. Cataract Refract. Surg.* **32**, 1860–1865 (2006).
- Linke, S. J., Steinberg, J., Eddy, M.-T., Richard, G. & Katz, T. Relationship between minimum corneal thickness and refractive state, keratometry, age, sex, and left or right eye in refractive surgery candidates. *J. Cataract Refract. Surg.* **37**, 2175–2180 (2011).
- Zhang, T. et al. Comparison of a new swept-source anterior segment optical coherence tomography and a Scheimpflug camera for measurement of corneal curvature. *Cornea* **39**, 818–822 (2020).
- Kim, E. J. et al. Repeatability of posterior and total corneal curvature measurements with a dual Scheimpflug-Placido tomographer. *J. Cataract Refract. Surg.* **41**, 2731–2738 (2015).
- Cerviño, A., Dominguez-Vicent, A., Ferrer-Blasco, T., García-Lázaro, S. & Albarrán-Diego, C. Intrasubject repeatability of corneal power, thickness, and wavefront aberrations with a new version of a dual rotating Scheimpflug-Placido system. *J. Cataract Refract. Surg.* **41**, 186–192 (2015).
- Shaw, A. J., Collins, M. J., Davis, B. A. & Carney, L. G. Eyelid pressure: Inferences from corneal topographic changes. *Cornea* **28**, 181–188 (2009).
- Montés-Micó, R., Cervino, A., Ferrer-Blasco, T., García-Lázaro, S. & Madrid-Costa, D. The tear film and the optical quality of the eye. *Ocul. Surf.* **8**, 185–192 (2010).
- Mohamed, M. et al. Repeatability and comparability of the Galilei-G4 and Cassini in measuring corneal power and astigmatism in normal and post-refractive surgery eyes. *Sci. Rep.* **11**, 16141 (2021).
- Poulsen, A. et al. Repeatability and reliability of a combined dual-Scheimpflug Placido disc corneal topographer in eyes with keratoconus. *Invest. Ophthalmol. Vis. Sci.* **60**, 2114–2114 (2019).
- Shetty, R. et al. Repeatability and agreement of three Scheimpflug-based imaging systems for measuring anterior segment parameters in keratoconus. *Invest. Ophthalmol. Vis. Sci.* **55**, 5263–5268 (2014).
- Lemp, M. A. & Foulks, G. N. The definition and classification of dry eye disease. *Ocul. Surf.* **5**, 75–92 (2007).
- Craig, J. P. et al. TFOS DEWS II definition and classification report. *Ocul. Surf.* **15**, 276–283 (2017).
- Read, S. A. & Collins, M. J. Diurnal variation of corneal shape and thickness. *Optom. Vis. Sci.* **86**, 170–180 (2009).
- Crawford, A. Z., Patel, D. V. & McGhee, C. N. Comparison and repeatability of keratometric and corneal power measurements obtained by Orbscan II, Pentacam, and Galilei corneal tomography systems. *Am. J. Ophthalmol.* **156**, 53–60 (2013).
- Moshirfar, M., Tenney, S., McCabe, S. & Schmid, G. Repeatability and reproducibility of the galilei G6 and its agreement with the pentacam® AXL in optical biometry and corneal tomography. *Expert Rev. Med. Dev.* **19**, 375–383 (2022).
- Wylegala, A., Mazur, R., Bolek, B. & Wylegala, E. Reproducibility, and repeatability of corneal topography measured by Revo NX, Galilei G6 and Casia 2 in normal eyes. *PLoS ONE* **15**, e0230589 (2020).
- Yokoi, N. et al. Classification of fluorescein breakup patterns: A novel method of differential diagnosis for dry eye. *Am. J. Ophthalmol.* **180**, 72–85 (2017).
- Zhu, M., Collins, M. & Iskander, D. Dynamics of ocular surface topography. *Eye* **21**, 624–632 (2007).
- King-Smith, E., Fink, B., Hill, R., Koelling, K. & Tiffany, J. The thickness of the tear film. *Current Eye Res.* **29**, 357–368 (2004).
- Menassa, N. et al. Comparison and reproducibility of corneal thickness and curvature readings obtained by the Galilei and the Orbscan II analysis systems. *J. Cataract Refract. Surg.* **34**, 1742–1747 (2008).
- Faramarzi, A., Karimian, F., Jafarinasab, M. R., Bonyadi, M. H. J. & Yaseri, M. Central corneal thickness measurements after myopic photorefractive keratectomy using Scheimpflug imaging, scanning-slit topography, and ultrasonic pachymetry. *J. Cataract Refract. Surg.* **36**, 1543–1549 (2010).
- Hashemi, H. & Mehravaran, S. Central corneal thickness measurement with Pentacam, Orbscan II, and ultrasound devices before and after laser refractive surgery for myopia. *J. Cataract Refract. Surg.* **33**, 1701–1707 (2007).
- Shirayama, M., Wang, L., Weikert, M. P. & Koch, D. D. Comparison of corneal powers obtained from 4 different devices. *Am. J. Ophthalmol.* **148**, 528–535.e521 (2009).
- Wang, L., Shirayama, M. & Koch, D. D. Repeatability of corneal power and wavefront aberration measurements with a dual-Scheimpflug Placido corneal topographer. *J. Cataract Refract. Surg.* **36**, 425–430 (2010).
- de Jong, T., Sheehan, M. T., Dubbelman, M., Koopmans, S. A. & Jansonius, N. M. Shape of the anterior cornea: Comparison of height data from 4 corneal topographers. *J. Cataract Refract. Surg.* **39**, 1570–1580 (2013).
- Aramberri, J. et al. Dual versus single Scheimpflug camera for anterior segment analysis: Precision and agreement. *J. Cataract Refract. Surg.* **38**, 1934–1949 (2012).

Author contributions

This study received no financial support. S.H. and M.H.K. had full access to the data and take overall responsibility for the study. Conception and design : Y.J.K., Y.U.S., M.H.K. Data collection : D.S.K., S.H., and D.K. Analysis and interpretation : E.H.H., D.S.K., S.H., M.H.K. Writing : S.H. Supervision : Y.J.K., M.H.K. All authors contributed substantially to the manuscript's revision.

Declarations

Competing interests

The authors declare no competing interests.

Additional information

Correspondence and requests for materials should be addressed to M.H.K.

Reprints and permissions information is available at www.nature.com/reprints.

Publisher's note Springer Nature remains neutral with regard to jurisdictional claims in published maps and institutional affiliations.

Open Access This article is licensed under a Creative Commons Attribution-NonCommercial-NoDerivatives 4.0 International License, which permits any non-commercial use, sharing, distribution and reproduction in any medium or format, as long as you give appropriate credit to the original author(s) and the source, provide a link to the Creative Commons licence, and indicate if you modified the licensed material. You do not have permission under this licence to share adapted material derived from this article or parts of it. The images or other third party material in this article are included in the article's Creative Commons licence, unless indicated otherwise in a credit line to the material. If material is not included in the article's Creative Commons licence and your intended use is not permitted by statutory regulation or exceeds the permitted use, you will need to obtain permission directly from the copyright holder. To view a copy of this licence, visit <http://creativecommons.org/licenses/by-nc-nd/4.0/>.

© The Author(s) 2024